

Density-functional study of impurity-related DX centers in CdF₂

Henry Pinto

Laboratory of Physics, Helsinki University of Technology, P. O. Box 1100, FIN-02015, HUT, Finland

and Centro de Investigación en Física de la Materia Condensada, Corporación de Física

Fundamental y Aplicada, Apartado 17-12-637, Quito, Ecuador

R M. Nieminen

Laboratory of Physics, Helsinki University of Technology, P. O. Box 1100, FIN-02015, HUT, Finland

We have studied computationally the CdF₂ crystal doped with Al, Ga, In, Sc and Y impurities, using the density-functional theory and the ultrasoft pseudopotential method. In particular, we focus on the bistability behavior of the dopants. The formation energies, ionization levels and spatial configurations are calculated. For bistable donor configurations (DX centers), the overlap populations and energy barriers are also estimated. The results obtained for the DX centers associated with Ga and In atoms in the negative charge state are in a good agreement with previous works. We predict the existence of bistability in the case of the Sc-doped CdF₂. In all the investigated cases for the DX-centers we find an antibonding state between the impurity and the nearest Cd atoms.

I. INTRODUCTION

The so-called DX-type dopant centers in semiconductors and insulators have been the subject of intensive because these centers have a number of important properties¹⁻⁷. One very special characteristic of the DX defects is their bistable behavior. This means that the defect possesses two equilibrium states separated by a vibronic energy barrier, namely, a shallow and a deep donor state, the latter accompanied by a large lattice relaxation²⁻⁴. The peculiarity of this type of defects is their presence not only in covalent crystals, e.g. III-V semiconductors¹⁻⁵, but also in ionic materials^{6,7}. In fact, some recent experimental measurements have demonstrated that the ionic CdF₂ crystal doped with trivalent impurities such as In and Ga shows bistability^{6,8,9}.

When In- or Ga- doped CdF₂ is exposed to UV-VIS radiation at low temperatures, the associated absorption peak disappears giving rise to an IR band^{6,8,9}. The explanation of this process is related to the electronic transfer from the deep state to the metastable shallow state due to photon absorption. It is also important to notice that the negative-effective-U nature of the deep-state has been confirmed by the quantum yield measurements⁶ at low temperatures, giving a value of $\sim 2e$ for the localised charge. This implies that the deep state contains two electrons. The electrons that were promoted to the shallow level cannot return to the deep state because of the energy barrier separating the states. The height of this barrier was experimentally estimated to be about 0.10 eV and 1.12 eV for In and Ga, respectively^{6,8,10}. Recently, positron annihilation experiments have revealed the existence of an open-volume defect related to the atomic configurations of the deep DX state in In- and Ga-doped CdF₂⁵.

Such DX behavior shows a large difference between the thermal and optical ionization energies (Stokes shift) observed in both DX:In and DX:Ga⁸. The electron photoionization in the deep state and its subsequent recapture into the shallow state causes a local change in the polarizability, thus changing the refractive index^{11,12}. This property enables one to use the material as efficient medium for the

optical storage of information with nanometer spatial resolution¹¹. It is also known that in Ga related DX centers, the metastable electron occupation exists up to 250 K¹² while for In the metastable electron occupation is observed only below 70K¹¹. This makes CdF₂:Ga a promising material for room-temperature operations. On the other hand, impurities such as Al and Y produce only shallow states.

In the present study we carry out *ab initio* computations using the total-energy plane-wave pseudopotential (PW-PP) method focusing on the DX behavior. The above-mentioned method allows us to estimate the formation energies and structural properties for both native defects and trivalent dopants. Additionally, we perform the Mulliken population analysis¹³ for trivalent bistable dopants. The predicted values for the formation energies of trivalent dopants with different charge states agree quite well with the recent theoretical studies by T. Mattila *et al.*¹⁴, as well as with the large lattice relaxations found by C. H. Park *et al.*¹⁵ in the case of Ga- and In-doped CdF₂. The latter work attributes the stability of the DX center associated with Ga or In in the negative charge state to the hybridization between *d* electrons of the impurity and *d* electrons of the Cd atom¹⁵. Our results point to the DX-behavior not only in the Ga- and In-dopants but also in the Sc-dopant. The geometry and the bond population analysis suggest that the interaction between the *d* electrons has an antibonding nature.

The manuscript is organized as follows. A detailed description of the computational methods and the reference results of bulk crystal calculations are given in Sec. II. The formation energies, geometries, local vibrations and population analysis are presented in Sec. III together with a discussion. Finally, in Sec. IV we give our conclusions.

II. COMPUTATIONAL DETAILS

The calculations are based on the density-functional theory (DFT) and the local-density approximation (LDA) as parametrized by Perdew and Zunger¹⁶ combined with the ultrasoft Vanderbilt

pseudopotential (PP) technique^{17,18}. Additionally, the density mixing scheme¹⁹ was used to minimize the Hohenberg-Kohn-Sham total-energy functionals. The use of ultrasoft pseudopotentials (USP) introduced by Vanderbilt has many advantages. It allows one to work with modest plane-wave (PW) energy cut-offs, and the generated PPs have exceptional transferability. Moreover, the use of USP allows one to treat explicitly the “shallow” core electrons in the calculations²⁰. This also adds high accuracy and transferability to the PP^{20,21}. Specifically, we have included as valence states the $2s$ state of F, the $4d$ state of Cd and In, the $3d$ state of Ga, and the $3s$, $3p$ and $3d$ states of Sc. We have found that using a PW cut-off of 25 Ry is sufficient to obtain well-convergent results for the CdF₂. The calculations were performed using the CASTEP computer code.^{17,21}

A. Perfect crystal

The perfect cadmium fluoride has a cubic structure ($Fm-3m$) with three atoms in its unit cell²². The experimental value of the band gap is found to be approximately 7.8 eV²³ and the lattice constant is equal to 5.356 Å²⁴. In order to calculate accurately the bulk crystal properties of perfect CdF₂, we have performed the computations using a 4x4x4 Monkhorst-Pack \mathbf{k} -point mesh²⁵. The predicted lattice constant of 5.338 Å is in a good accordance with the experimental value and previous theoretical estimations of 5.307 Å¹⁴ and 5.354 Å¹⁵. Furthermore, our estimation of 1.25 Mbar for the bulk modulus agrees very well with the earlier computed values of 1.21 to 1.30 Mbar¹⁴ and 1.27 Mbar¹⁵. We have also calculated the one-electron band structure of CdF₂. Figure 1 shows a visual comparison of our results for CdF₂ with those of Ref. 14. As it is possible to appreciate, there is no significant difference. From our calculations, the indirect band gap is estimated to be 2.89 eV, which is considerably smaller than the experimentally obtained value of 7.8 eV. This underestimation is a typical limitation of the DFT/LDA methods. However, as only total-energy differences are considered in the following, we do not expect the gap error to seriously affect the conclusions of this work.

B. Defective crystal

To minimize the artificial effect introduced by the mutual defect-defect interactions when the supercell model is used, the calculations were performed using bcc supercell consisting of 48 atoms spanned by the following lattice vectors: (1,1,-1), (-1,1,1), (1,-1,1). Due to its large size this supercell together with the $1/4(1,1,1)$ \mathbf{k} -point mesh for the reciprocal space integration is expected to have zero closest-defect interaction²⁶. Additionally, for the cases of Ga- and Sc-doped CdF₂, we have carried out computations with several supercells with different geometries and \mathbf{k} -point meshes, keeping the same number of atoms.

C. Formation energies and population analysis

Throughout the study, the formation energy of a defect in a given charge state q , $E_f(q)$, is calculated by the standard procedure^{14, 27, 28}

$$E_f(q) = E_D(q) + q(E_v + \mu_e) - \sum_i n_i \mu_i \quad (1)$$

where E_D is the total energy of the defective supercell, E_v the maximum energy value of the upper valence band in the perfect CdF₂ (at the \mathbf{W} point), and μ_e is the electron chemical potential relative to the band maximum. Finally, n_i and μ_i stand for the number of atoms of type i and its chemical potential, respectively. Due to the defect-defect interactions arising from finite supercell size, the error introduced in the E_v is corrected by using the so-called average potential correction^{29,30}.

The atomic chemical potentials of the host constituents, Cd and F, fulfill the following equation
Thus we can consider the effect of growth conditions. The Cd-rich conditions correspond to μ_{Cd}

calculated from hexagonal Cd metal²² and inserting the value in Eq. (2) and solving for μ_F . For the F-rich conditions we have to use μ_F calculated for the F_2 -dimer. In the case of the impurities, their atomic chemical potentials are obtained by calculating the formation energies for the relevant starting material constituents¹⁴. The compounds utilized also in the present work, InF_3 , GaF_3 and AlF_3 ,²² were suggested in Ref. 14. The ionization levels are calculated from the magnitudes of Fermi level μ_e , at which energies of the competing charge states cross²⁰. The ionization levels can be obtained by solving for u_e from the following equation

$$E_D(q) + q(E^{q_v} + \mu_e) = E_D(q') + q'(E^{q'_v} + \mu_e) \quad (3)$$

Because of the fact that the total energy values are less influenced than the Kohn-Sham single-particle eigenvalues by the LDA approximation, we allow μ_e to vary within the full experimental band gap.

The Mulliken population analysis¹³ for the PW-PP calculations was carried out using the scheme described in Refs. 31-32. Within this technique the eigenfunctions are projected onto a basis set comprised of a linear combination of atomic orbitals^{31,32}. Basically, the projection calculates both the density matrix $P_{\sigma\mu}(k)$ and the overlap matrix $S_{\sigma\mu}(k)$ for the localised basis set. Within this scheme, the Mulliken charge $Q_m(A)$ associated with an atom A is given by

$$Q_m(A) = \sum_k w_k \sum_{\sigma}^{\sigma \in A \vee A} \sum_{\nu} P_{\sigma\nu}(k) S_{\sigma\nu}(k) \quad (4)$$

and the overlap population $n_m(AB)$ between the atoms A and B is computed as

$$n_m(AB) = \sum_k w_k \sum_{\sigma}^{\sigma \in A \vee B} \sum_{\nu} 2P_{\sigma\nu}(k) S_{\sigma\nu}(k) \quad (5)$$

In the last two equations, w_k are the weights associated with the \mathbf{k} -points in the Brillouin zone. It is important to mention that the quality of the projections is determined by the calculation of the so-called

splitting parameter³¹. It is a parameter that varies between 0 and 1 and measures the ability of a basis set to represent PW states, e.g., it is zero when projected wave functions perfectly represent the PW states and 1 if the atomic basis set is orthogonal to the PW eigenstates. This technique is very useful to study the variation of the covalent bonding of the DX centers in the CdF₂.

III. RESULTS AND DISCUSSION

A. Energetical, structural and electronic properties of shallow states

We have calculated the enthalpy of formation for pure cadmium difluoride considering its elemental precursors (hexagonal Cd and F₂ dimers) as mentioned in Sec. II. The calculated value was found to be -8.56 eV, which is close to the experimentally known value of -7.26 eV³³. The difference reflects the tendency of the LDA approach to overestimate the cohesion energy of solids.

The results for group-III impurities Al, Ga, and In as well as those for group-II impurities Sc and Y are presented in Table I. In the case of the three first impurities, we find the negative-effective-U character, i.e. the positive and negative charge states are always more stable than the neutral state. This result is in accordance with the experimental quantum yield measurements for the In-doped CdF₂⁶.

On the other hand, we find that when the CdF₂ is doped with Sc, the impurity exists in a singly positive charge state or in the DX form as a negative charge state. This will be discussed below in more detail.

In general, the ionization levels show a tendency to occur more or less in the middle of the band gap. In Table II the relaxations around each calculated impurity in their negative or positive charge states are presented. We have considered the atomic displacements with the impurity atom fixed to its substitutional position. In the perfect CdF₂ lattice eight F atoms surround the impurity (see Fig. 2). The distances d_i are the atomic distances between the impurity and a given F atom. As seen from Table II, the Al and Ga atoms show a similar behavior in the negative charge state because F_i ($i=1-4$) show an

inward relaxation (26%) while the remaining F atoms experience outward relaxations (12%). In the case of the In impurity, we find a negligible relaxation in the negative charge, with the nearest-neighbor inward relaxation equal to 5%. These results are in good agreement with those obtained previously by T. Mattila *et al.*⁵ The percentage values are given with respect to the F-Cd inter-atomic distance, 2.631 Å, in the perfect lattice.

B. Occurrence of the DX behavior in Ga-, In- and Sc-doped CdF₂

In order to examine the bistable behavior of impurity-doped CdF₂, we next allow for the displacements of the Ga, In and Sc atoms situated inside the cube formed by eight F atoms along the [100] axes (see Fig. 3). The relaxations were performed similarly as in previous studies of similar kind of defects^{4,34,35}, where very large atomic movements were reported.

Our results reveal that additionally to the expected bistability in Ga- and In-doped CdF₂ as suggested by C. H. Park *et al.*⁴, Sc-doped CdF₂ also exhibits bistability when the Sc complex is in a negative charge state. We have also used the same optimisation technique to the Al impurity. However, it was found that the Al impurity always returns to its normal substitutional position upon relaxation. In order to see possible artificial effects introduced by the defect-defect interactions, we have also performed several calculations for a series of 48-atom supercells using suitable **k**-points for the reciprocal integration (see Table III). We have also performed the same calculations for both Ga and Sc impurities in order to compare the values for the barrier separating the two potential minima. During the lattice relaxation we have considered 18 atoms including the impurity (see Fig. 3). It is important to notice that the inclusion of Sc *3s*, *3p* and *3d* states as valence electrons made our calculations very accurate. So far there is no experimental confirmation of the existence of DX centers in case of the Sc impurity.

When the bcc supercell with the 1/4 (1,1,1) **k**-point sampling is used, we find the second

potential minimum for Sc, accompanied by large lattice relaxation. The magnitude of the stable displacement for the Sc atom is found to be equal to 2.41 Å. In contrast, the minimum-energy displacement for the Ga atom impurity is found to be equal to 1.84 Å for the bcc supercell and 1.87 Å for the case of the tetragonal (T1) supercell. When we then carry out the relaxation procedure in the tetragonal supercell and the Γ -point, we cannot find any bistability for either Ga- or Sc-doping. However, if we use the T2 supercell together with 4 \mathbf{k} points (the 2x2x2 Monkhorst-Pack grid), both the Sc and Ga impurities exhibit bistability with the atomic displacements equal to 2.23 Å and 1.66 Å, respectively. Thus we can conclude that Sc-doped CdF₂ shows bistable behavior.

After a careful study of the bistability in the Sc-doped CdF₂ crystal, we have proceeded to compute the energetical, structural and chemical properties of the DX centers associated with Ga, In and Sc, using an 48-atom bcc supercell with the 1/4 (1,1,1) \mathbf{k} -point mesh as mentioned in the Sec. II. The corresponding results are given in Tables IV and V as well as in Fig. 3.

In and Ga impurities produce a total outward relaxations of the atoms surrounding the impurity, e.g., as is shown in Fig. 3a. It is interesting to notice that the F(1) atoms have considerable displacements of about 6% for the DX:Ga, DX:In and DX:Sc. The percentages are given with respect to the F-Cd initial inter-atomic distance (2.631 Å) in the perfect crystalline lattice. In Table IV we show detailed information for the lattice relaxation.

The displacements for the In and Ga impurities were found to be equal to 1.95 Å (74%) and 1.85 Å (70 %), respectively. These outcomes are in good agreement with the values of 1.82 Å (Ga) and 1.84 Å (In) found in Ref. 4. It is interesting to relate our results of the lattice relaxation with the experimental results obtained by Nissilä *et al.*⁷ Their work revealed the existence of open volume regions associated with DX:Ga and DX:In, implying large lattice relaxations.

In the case of the DX:Sc, the Sc impurity has the displacement of 2.41 Å (92%) and the eight-nearest F atoms have an inward relaxation of 0.23 Å (8.7%) for the F(3)-atoms and 0.1 Å (3.8%) for the

F(2)-atoms, while the remaining atoms present an outward relaxation as is shown in detail in Fig. 3.b and Table IV.

The energetic properties and chemical character of the DX centers are presented in Table V. The values obtained for the formation energies of the DX centers show clearly the negative-effective-U character.

The energy levels of the deep states with respect to the valence band maximum (VBM) are at 2.5 eV, 2.61 eV and 2.3 eV for the Ga, In and Sc impurities, respectively. The wave function of these levels is rather dispersed around the F(1)-atoms.

The population analysis has been carried out for both the defective and perfect supercells, in order to facilitate comparison. The results from the perfect supercell display the overlap population of 0.12 and -0.06 for the Cd-F and the F-F bonds, respectively. Positive and negative values of n_m indicate bonding and antibonding states, respectively³². The bond population n_m of the four nearest Cd atoms with the impurity atom were found to be -2.23 (Ga-Cd), -1.5 (In-Cd) and -0.14 (Sc-Cd) (see Table V and Fig. 3 for more details). In these estimations, the value of the splitting parameter is around 0.001, which is sufficiently small for a good description³². The results for the defective region clearly show an increase in the covalency, in accordance with previous studies³⁶. The obtained negative values point out to the fact that the $d-d$ interaction is repulsive in contrary to the suggestion in Ref. 4.

This unexpected result opens the problem of stability for the DX centers in CdF₂ and encourages us to propose an alternative model to explain the observed behavior: the negative values of the bond population for the Ga, In or Sc interacting with the nearest Cd atoms is difficult to reconcile with the large displacements of the impurities.

We have mapped the total energy surface for the impurity atoms, Ga and In, displaced along the [100] axis (Fig. 5). The estimated energy barriers for the shallow-deep transition were found to be 1.5 eV and 2.13 eV for the Ga and In, respectively as shown in Table V. The result of 1.5 eV is in

accordance with the previous theoretical (1.0 eV)⁴ and experimental (1.24 eV)⁶ results.

We suggest that the bistability with large displacements is due to the competition between the attractive electrostatic (dipolar) interactions generated by the electronic redistribution/large displacements on one side and the covalent $d-d$ repulsion of the impurity (Ga, In, Sc) with the nearest Cd atoms on the other. We would thus conclude that the Al impurity does not present bistability because there are no d -electrons, as already argued in Ref. 15.

IV. CONCLUSIONS

We have performed first-principles pseudopotential calculations for CdF₂ crystals doped with Al, Ga, In and Sc impurities. We have calculated the formation energies, ionization levels, geometries, energy barriers and bond populations, focusing on the bistability question. The results for the normal site location of the impurities are in good agreement with a number of recent theoretical studies^{14,15}. We have found the existence of bistability for Ga, In and Sc impurities when they are in the negative charge state. Our results for the geometry of the DX centers clearly exhibit the open volume type of defects, in accordance with experiments using e positron annihilation⁷. The estimated energy barrier for the DX:Ga is in good agreement with both experimental⁶ and another *ab initio* study⁴. We have found the existence of an antibonding state between the impurity (In, Ga and Sc) and the four surrounding Cd atoms. We suggest that the competition of the attractive electronic polarization along the [100] axis and the covalent repulsive interaction between the nearest Cd with the impurity stabilizes the DX center in the Ga-, In- and Sc-doped material. We also conclude that the formation of the DX centers requires the existence of d electrons, because no bistability is observed in Al-doped CdF₂.

ACKNOWLEDGMENTS

This work has been supported by the Academy of Finland through the Centers of Excellence Program (2000-2005). H. Pinto acknowledges the support from the Center of International Mobility (CIMO) in Finland. The authors would like to acknowledge the generous computational resources of the Center for the Scientific Computing (CSC), in Espoo, Finland.

References

1. P. M. Money, J. Appl. Phys. **67**, R1 (1990).
2. D.J. Chadi and K. J. Chang, Phys. Rev. B **39**, 10063 (1988).
3. R. A. Linke, I. Redmond, T. Thio, and D.J. Chadi, J. Appl. Phys. **83**, 661 (1998).
4. C.H. Park and D. J. Chadi, Appl. Phys. Lett. **66**, 3167 (1995)
5. T. Mattila and R.M. Nieminen, Phys. Rev. B **54**, 16676 (1996)
6. A. S. Shcheulin, A.I. Ryskin, K. Swiatek and J.M.Langer, Phys. Lett. A **222**, 107 (1996).
7. J. Nissilä, K. Saarinen, P. Hautojärvi, A. Suchocki and J.M. Langer, Phys. Rev. Lett. **82**, 3276 (1999).
8. J. E. Dmochowski, J. M. Langer and Z. Kalinski, Phys. Rev. Lett. **56**, 1735 (1986).
9. J. E. Dmochowski, W. Jantsch, D. Dobosz and J. M. Langer, Acta. Phys. Pol. A **73**, 247 (1988).
10. A. I. Ryskin, A. S. Shcheulin and D. E. Onopko, Phys. Rev. Lett. **80**, 2949 (1998).
11. A. I. Ryskin, A. S. Shcheulin, B. Koziarska, J. M. Langer, A. Suchocki, I. I. Buczinskaya, P. P. Fedorov and B. P. Sobolev, Appl. Phys. Lett. **67**, 31 (1995).
12. A. Suchocki, B. Koziarska, T. Langer and J. M. Langer, Appl. Phys. Lett. **70**, 2934 (1997).
13. R. S. Mulliken, J. Chem. Phys. **23**, 1833 (1955).
14. T. Mattila, S. Pöykkö and R.M. Nieminen, Phys. Rev. B **56**, 15665 (1997).
15. C. H. Park and D.J.Chadi, Phys. Rev. Lett **82**, 113 (1999).
16. J. Perdew and A. Zunger, Phys. Rev. B. **23**, 5048 (1981).
17. M. C. Payne, M. P. Tarter, D.C. Allan, T. A. Arias, and J. D. Joannopoulos, Rev. Mod. Phys. **64**, 1045 (1992).
18. D. Vanderbilt, Phys. Rev. B **41**, 7892 (1990).
19. G. Kresse and J. Furthmüller, Phys. Rev. B **54**, 11169 (1996).

20. R. D. King-Smith and D. Vanderbilt, *Phys. Rev. B* **49**, 5828 (1994).
21. V. Milman, B. Winkler, J. A. White, C. J. Pickard, M. C. Payne, E. V. Akhmatkaya, and R. H. Nobes, *Int. J. Quant. Chem.* **77**, 895 (2000).
22. W. G. Wyckoff, *Crystal Structures* (Interscience Publishers, New York, 1963).
23. B. A. Orlovski and P. Pleniewicz, *Phys. Status Solidi B* **126**, 285 (1984).
24. O. Madelung, M. Shulz and H. Weiss, *Landolt-Börnstein Tables*, (Springer, Berlin, 1984).
25. H. J. Monkhorst and J.D. Pack, *Phys. Rev. B* **13**, 5188 (1976).
26. G. Makov, R. Shah, and M. C. Payne, *Phys. Rev. B* **53**, 15513 (1996).
27. G. -X. Qian, R. M. Martin, and D. J. Chadi, *Phys. Rev. B* **38**, 7649 (1988).
28. S. B. Zhang and J. E. Northrup, *Phys. Rev. Lett.* **67**, 2339 (1991).
29. S. Pöykkö, M. J. Puska, and R. M. Nieminen, *Phys. Rev. B* **53**, 3813 (1996)
30. K. W. Kwak, D. Vanderbilt, and R. D. King-Smith, *Phys. Rev. B* **52**, 11912 (1995).
31. D. Sanchez-Portal, E. Artacho and J. Soler, *J. Phys.:Condes. Matter* **8**, 3859 (1996).
32. M.D. Segall, R. Shah, C. J. Pickard, and M. C. Payne, *Phys. Rev. B* **54**, 16317 (1996).
33. *CRC Handbook for Chemistry and Physics*, 80th ed. (CRC, Boca Raton, 1999).
34. T. Mattila and R. M. Nieminen, *Phys. Rev. B* **54**, 16676 (1996).
35. T. Mattila and R. M. Nieminen, *Phys. Rev. B* **55**, 9571 (1997).
36. D. E. Onopko and A. I. Ryskin, *Phys. Rev. B* **61**, 12952 (1999).

TABLE I. Calculated ionization levels (eV) and formation energies E_f (eV) at these ionization levels for both F-rich and Cd-rich conditions. The $\text{CdF}_2\text{:Sc}$ and $\text{CdF}_2\text{:Y}$ were found to be stable only in the singly positive charge state.

Defect	(-/+)	Cd-rich	F-rich
$\text{CdF}_2\text{:Al}$	3.27	1.7	5.7
$\text{CdF}_2\text{:In}$	3.16	-1.2	3.1
$\text{CdF}_2\text{:Ga}$	3.31	1.15	4.3

TABLE III. Results of the existence of DXcenters using different \mathbf{k} -point sets and several supercell geometries: bcc, tetragonal (T1) with lattice vectors (2,0,0); (0,2,0); (0,0,1), and tetragonal (T2) with lattice vectors (1,1,0), (-1,1,0), (0,0,2). d_{DX} is the displacement in Å of the impurity with respect to its expected substitutional position.

Supercell-geometry	\mathbf{k} -point	DX existence	d_{DX}
bcc:Ga	1/4 (1,1,1)	Yes	1.84
T1:Ga	Γ	Yes	1.87
T2:Ga	Γ	No	
T2:Ga	($\pm 1/4, \pm 1/4, \pm 1/4$)	Yes	1.66
bcc:Sc	1/4 (1,1,1)	Yes	2.41
T1:Sc	Γ	Yes	2.11
T2:Sc	Γ	No	
T2:Sc	($\pm 1/4, \pm 1/4, \pm 1/4$)	Yes	2.23

TABLE IV. Displacements in Å for the DX centers for: Ga, In and Sc. The F(i)'s represent four F atoms laying in the plane perpendicular to the direction of impurity displacement. A negative value indicates an inward displacement.

	$\Delta d_{F(1)}$	$\Delta d_{F(2)}$	$\Delta d_{F(3)}$	$\Delta d_{Cd-nearest}$	d_{DX}
DX:Ga	0.17	0.09	0.04	0.07	1.84
DX:In	0.17	0.20	0.05	0.12	1.95
DX:Sc	0.15	-0.10	-0.23	0.19	2.41

TABLE V. Calculated impurity energy-levels E_{level} (eV) , ionization levels (+/-) in eV, overlap population between the impurity and the four-nearest Cd atoms $n_{\text{cd-imp}}$ and energy barriers E_b (eV) for the bistable configurations with Ga, In and Sc. A negative value of $n_{\text{cd-imp}}$ implies an antibonding state.

	E_{level}	(+/-)	$n_{\text{cd-imp}}$	E_b
DX:Ga	2.5	4.05	-2.23	1.5
DX:In	2.61	4.31	-1.5	2.13
DX:Sc	2.3	4.43	-0.14	

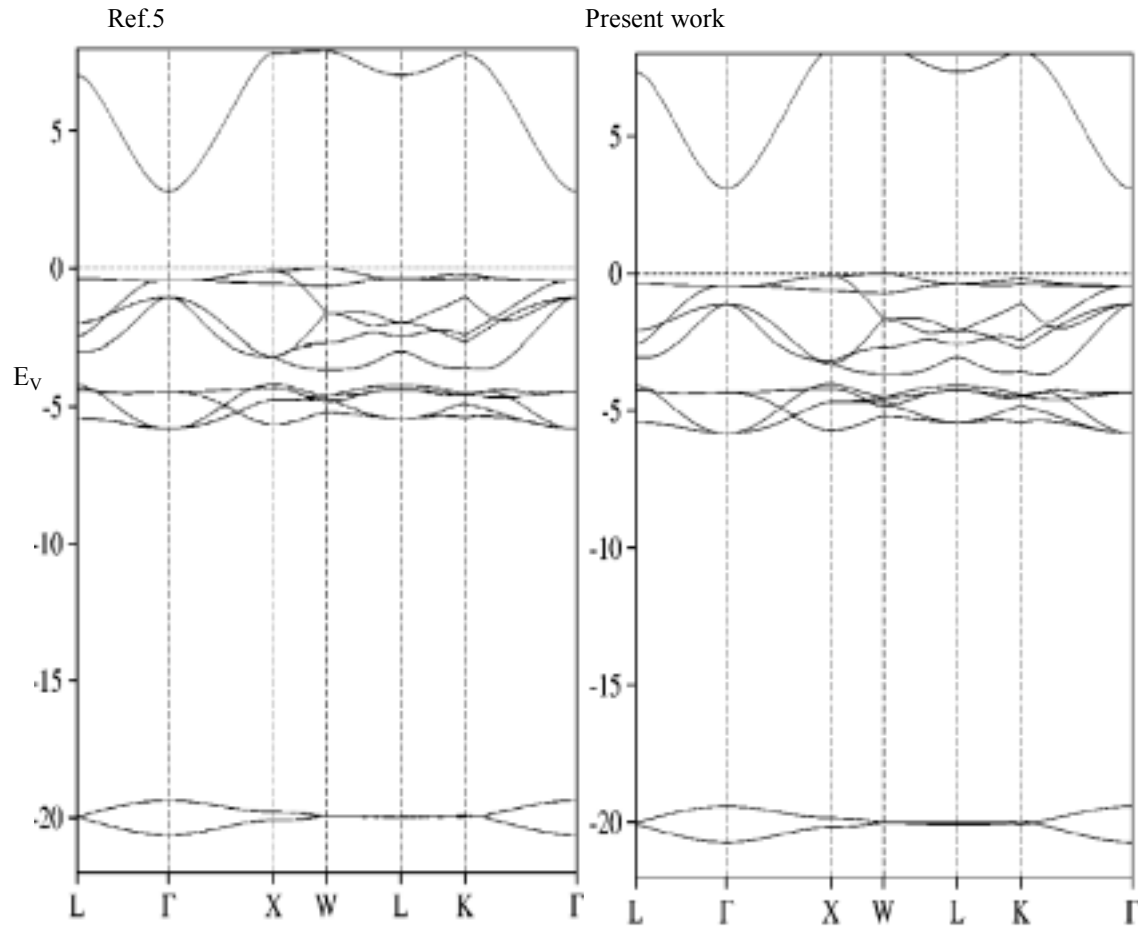


Fig.1. Comparison of band structures obtained by Mattila et. al. (Ref. 5) and the present results using USPP for the CdF₂ crystal.

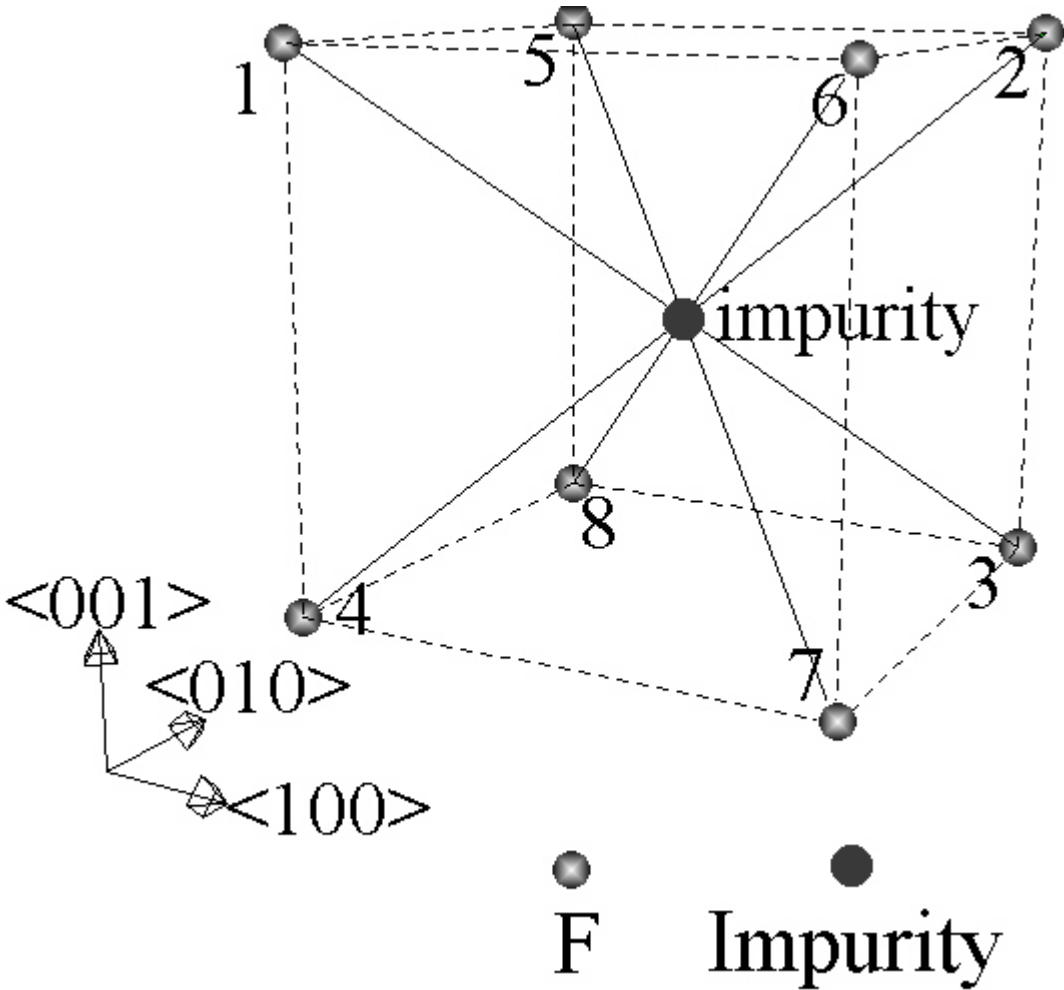


Fig.2. Arrangement of the nearest F atoms to the impurity (Al, In, Sc, Ga, Y).

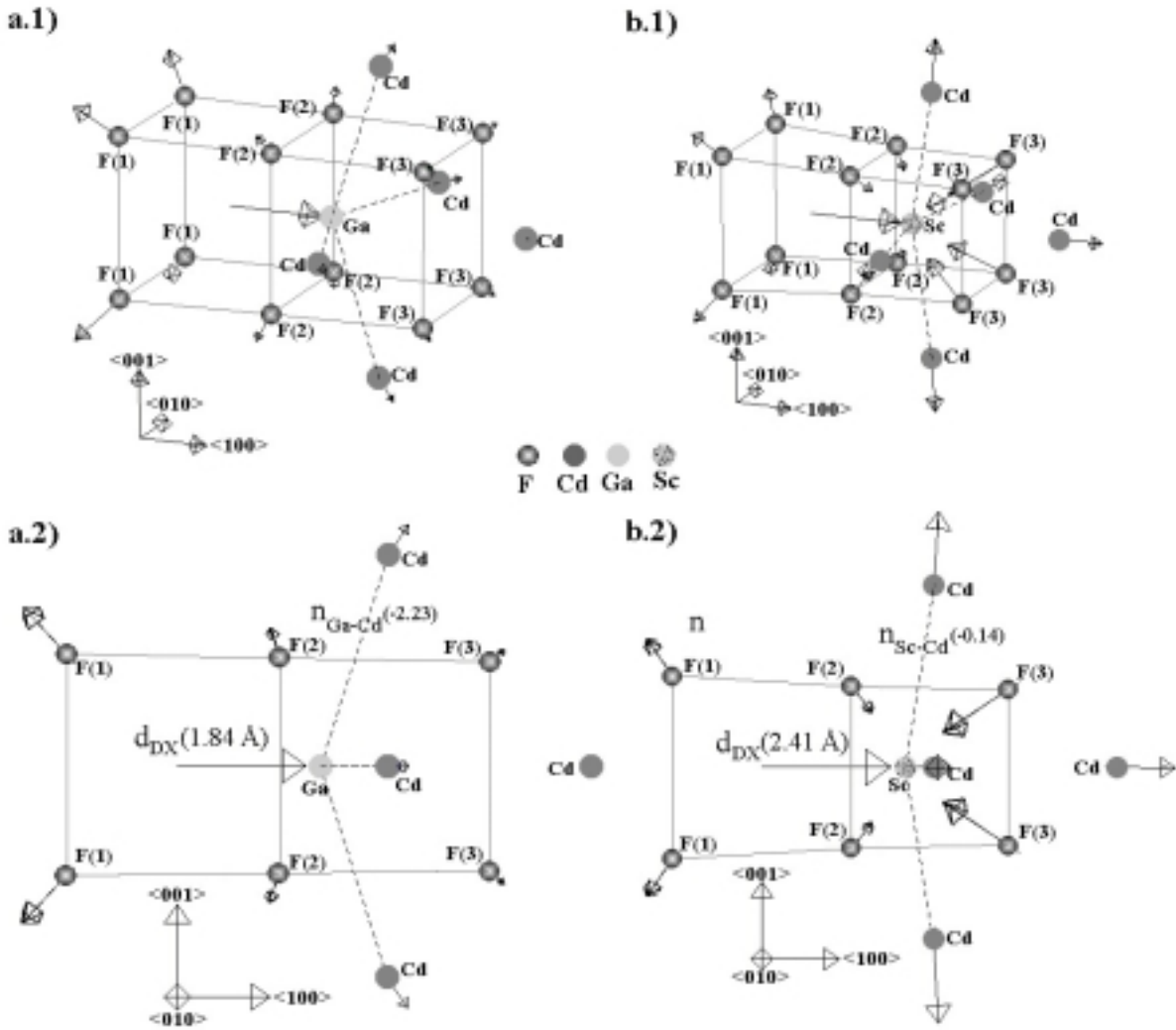


Fig.3. Detailed information of the relaxations for two systems: a) DX:Ga and b) DX:Sc. The figures a2) and b2) are plots viewed from the $\langle 010 \rangle$ axis. It is important to notice that for the Ga and In cases, all the nearest F atoms have outward relaxations while for the Sc case, the F(3) and F(4) atoms have an inward relaxation. Also the values of the bond population $n_{\text{Ga-Cd}}$ (-2.23) and $n_{\text{Sc-Cd}}$ (-0.14) are marked. The magnitude of the impurity displacement are also indicated. All the displacement arrows are magnified by a factor of seven, except for the displacement of the impurity.

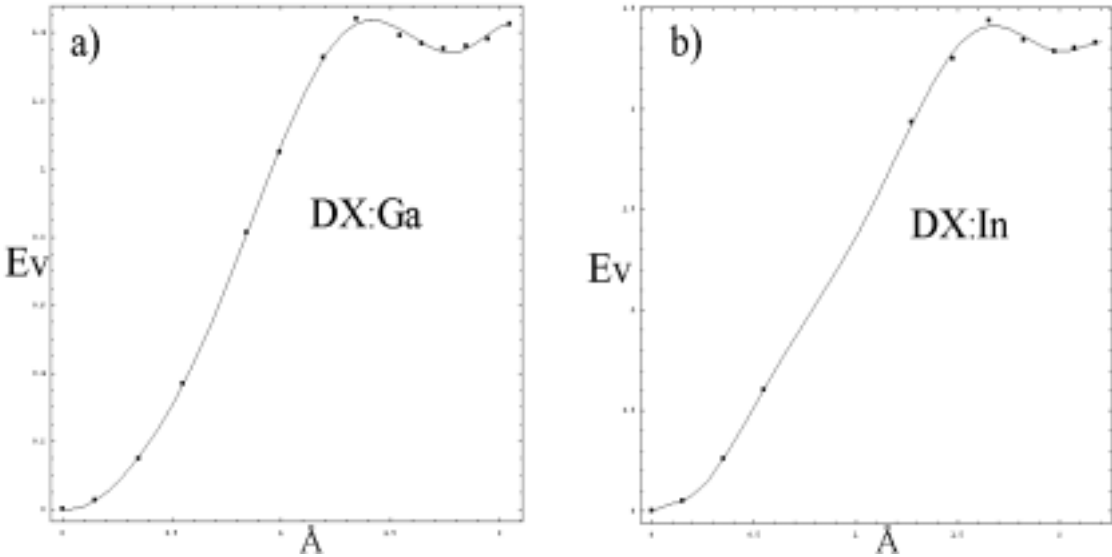


Fig.4. The total energy as a function of the dopant displacement for a) Ga and b) In, along the <100> axis.